LAWRENCE
LIVERMORE
NATIONAL
LABORATORY

UCRL-JRNL-209599

Proton Fast Ignition

M. H. Key, R. R. Freeman, S. P. Hatchett, A. J. MacKinnon, P. K. Patel, R. A. Snavely, R. B. Stephens

February 10, 2005

Proton Fast Ignition

Disclaimer

PROTON FAST IGNITION

M. H. Key[1], R. R. Freeman[2], S. P. Hatchett[1],
A. J. MacKinnon[1], P. K. Patel[1], R. A. Snavely[1], R. B. Stephens[3]

[1]Lawrence Livermore National Laboratory, Livermore, CA 94550, USA
[2]Ohio State University, Columbus, OH 43210, USA
[3]General Atomics, San Diego, CA, USA 92186, USA

Abstract

Fast ignition (FI) by a laser generated ballistically focused proton beam is a more recently proposed alternative to the original concept of FI by a laser generated beam of relativistic electrons. It has potential advantages in less complex energy transport into dense plasma. Recent successful target heating experiments motivate further investigation of the feasibility of proton fast ignition. The concept, the physics and characteristics of the proton beams, the recent experimental work on focusing of the beams and heating of solid targets and the overall prospects for proton FI are discussed.

1 Introduction

Inertial confined fusion (ICF) is the major alternative to magnetic confined fusion. The indirect and direct drive approaches to ICF have been reviewed respectively by Lindl et al.(1995 and 2004)[1] and Bodner (1998)[2]. Both rely on implosion of a spherical shell of deuterium –tritium ice with a central core of D-T gas to compress and ignite the fuel at a central hot spot. Fast ignition (FI) is a newer approach to ICF proposed in outline by Basov et al (1992)[3] and in much fuller detail by Tabak et al. (1994)[4]. Fuel compression and ignition are separated in FI by using a shell of fuel at solid density which is compressed by long pulse beams, together with short duration localized heating and ignition of the compressed fuel by a short pulse laser beam .as illustrated schematically in figure1.

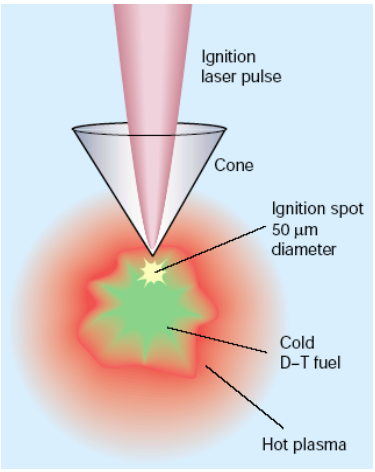

Figure 1. The fast ignition concept using implosion of a spherical shell with an inserted hollow cone to provide a path for the ignition laser pulse to generate electrons close to the compressed D-T plasma

The original concept of Tabak et al. assumed the short pulse laser beam would penetrate close to the dense fuel through a laser formed channel in the plasma and that laser generated relativistic electrons would ignite the fuel A variant concept was developed in hydrodynamic designs by Hatchett et al[5] and in experiments and hydrodynamic designs by Kodama et al (2001 and 2002)[6]. This variant recognized that laser beam would have great difficulty penetrating the long scale length of increasing plasma density outside the dense core. As shown in Figure 1, they used a hollow cone to protect the path of the ignitor laser beam. The results of the experiments of Kodama et al were a significant landmark for fast ignition,[7]and suggested that the short pulse ignitor laser could couple energy to the ignition hot spot with >20% efficiency.

The requirements for ignition have been modeled in detail by Atzeni (1999)[8] leading to the following analytic scalings for the energy, power and intensity of the ignitor electron beam required to heat the ignition hot spot of density x radius of 0.5 gcm^{-2} to the ignition temperature of 10 keV;

$$E_{ig} = 140\left(\frac{\rho}{100\ \mathrm{g/cm^3}}\right)^{-1.85}\ \mathrm{kJ},$$

$$W_{ig} = 2.6\times 10^{15}\left(\frac{\rho}{100\ \mathrm{g/cm^3}}\right)^{-1}\ \mathrm{W},$$

$$I_{ig} = 2.4\times 10^{19}\left(\frac{\rho}{100\ \mathrm{g/cm^3}}\right)^{0.95}\ \mathrm{W/cm^2}.$$

Equations 1

These requirements are for the laser generated fast electron beam reaching the dense core without regard to any possible losses in the transport to the dense core. As an example, they imply (for core density values of 300 gcm^{-3}) specifications of the electron beam of 20kJ, 0.9 PW, and $7x10^{19}Wcm^{-2}$.

FI has potentially important advantages over hot spot ignition, which include higher, gain (the ratio of fusion energy output to energy used to induce the fusion burn) and reduced energy required to reach the ignition threshold[9]. The optimum density for high gain and a manageable scale of total energy is about $300gcm^{-3}$, the density sets the ignitor requirements from Equations 1. The implosion driver has less stringent constraints due to relaxed requirements for spherical symmetry and for final pressure and density in the compression of the fusion fuel. Greater tolerance of surface finish imperfections in the fuel capsule makes target fabrication easier. A further feature is that FI can be used with any of the ICF fuel compression schemes currently being developed, which include direct drive with laser beams and indirect drive using thermal x-rays in holhraum enclosures

heated by either laser beams, ion beams or Z pinches. These advantages all contribute to making FI an attractive possibility for a fusion energy power plant.

Proton fast ignition was first proposed by Roth et al in 2001[10]based on the first observations of the then new phenomenon (discussed here later) of intense collimated emission of >10MeV protons (accompanied by neutralizing electrons) from the rear surface of a thin foil target irradiated on its front surface by a focused PW laser beam. The possibility of using a concave spherical target surface to focus the protons with the proton beam then serving, as the ignitor in fast ignition is the central concept illustrated in figure 2.

The key potential advantage in using proton beams lies in their energy transport which is expected to be relatively immune to the complex collective modifications of spatial and angular pattern of transport by self generated E and B fields, The mass ratio of the proton relative to the electron produces the attractive stiffness of the proton beam. A second advantage is avoidance of any lack of self-consistency in the laser intensity requirements for optimum electron energy and for the laser intensity needed to generate the required ignitor electron beam intensity, which is a potential problem in electron fast ignition.

2 Requirements for proton ignition

The first estimates of the proton beam requirements for ignition by Roth et al., used proton energy loss rates in cold matter. This simplification resulted in an estimate of 15 to

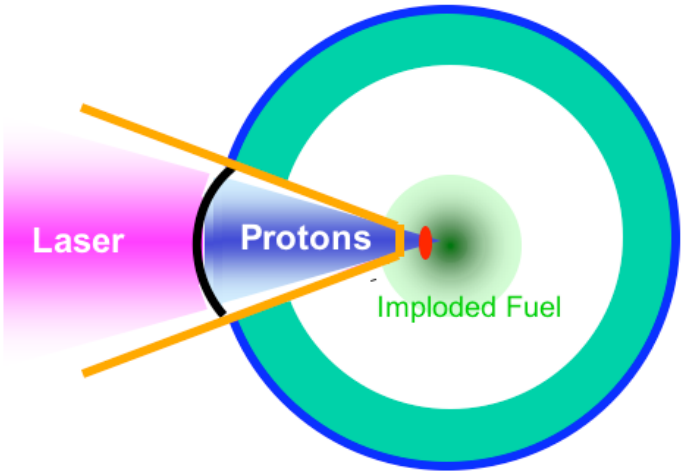

Figure 2. The proton fast ignition concept. A D-T shell target is imploded around a cone and a focused proton beam ignites the compressed plasma. The cone angle could at one extreme be 180° with a hemi- shell implosion and a hemi- shell proton source (the latter having been used in successful proton focusing experiments discussed later). A narrower cone angle may be preferred for the implosion hydrodynamics provided the proton focusing, not yet demonstrated in such geometry, could be accomplished.

23 MeV for the proton particle energies needed to heat the 0.5 gcm^{-2} (density) x (radius) product of the ignition hot spot. Included in the model was the spread of arrival time for protons of different energy, which is a limiting factor on the distance of the ignition hot spot from the proton generating foil. The time spread must be less than the typically 20 ps inertial confinement time of the hot spot. Roth et al. concluded that a narrow range of proton energies was necessary because of differences in arrival time due to an assumed 4mm distance between the proton source and the hot spot.

Subsequent more detailed modeling of the ignition process by Atzeni, Temporal and Honrubia (2002)[11] included the change of proton range with temperature of the heated DT target as shown in figure 3. Apparent in the figure is that a 15 MeV proton has a range of 0.6 gcm^{-2} in cold DT whereas a 3 MeV proton has the same range if the temperature is raised to 6 keV. A fortunate consequence is that faster protons arriving earlier have the necessary range to heat the hot spot in the cold target but slower protons arriving later encountering a heated target, also have sufficient range to add to the heating of the hot spot. This reduces the lower limit on useful proton energies and increases the spread of useful energies, which is important since the proton source as discussed later, has a broad quasi –exponential energy spectrum.

Numerical modeling of ignition of a uniform sphere of 100 m radius at 400 g/cc by a cylindrical proton beam of radius 15 m was carried out by Atzeni et al., for Boltzmann energy spectra as a function of the average energies (temperatures) of the protons, for various source to hot spot distances and also for mono-energetic protons. A much more favorable conclusion on the energy required in proton beam was reached as shown in figure 4. The requirements for ignition show a rather wide range of tolerable proton beam temperature and a considerable advantage for shorter propagation distances e.g. 1mm propagation and 3MeV temperature giving ignition with only 16 kJ of protons as shown in figure 4. Assuming a 20 ps pulse, where the protons heat the ignition spot the density of the protons is $1.4x10^{23}cm^{-3}$. The un-neutralized current is 267 MA which is 31x the proton Alfven current indicating that there must also be current neutralization for proton ignition as is the case for electron ignition.

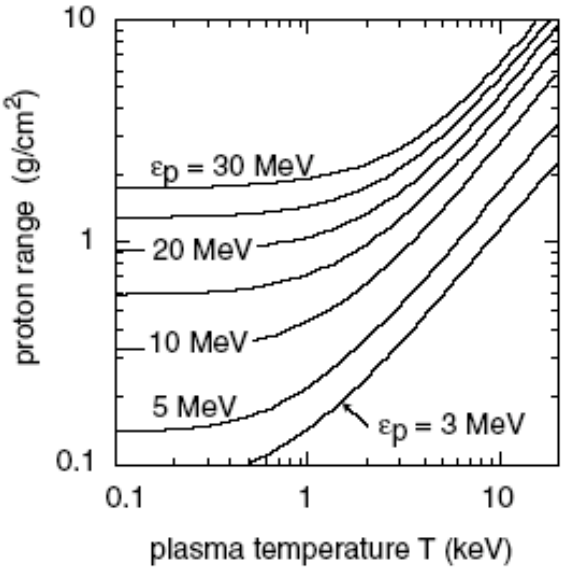

Figure 3. Proton range in heated D-T fuel (from Atzeni et al 2002)

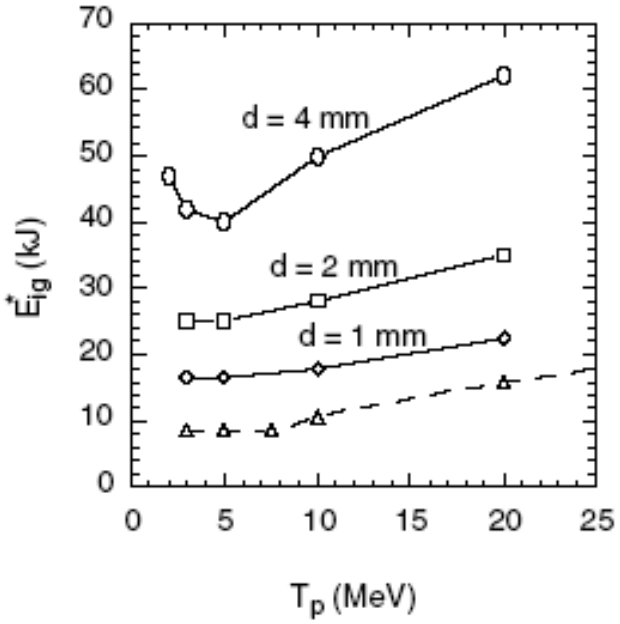

Figure 4. Minimum beam energy E_{ig} for fast ignition of a pre-compressed homogeneous DT sphere (with density = 400 gcm^{-3} and radius R = 100 m) by protons with exponential energy distribution and average energy T_p, originated at a distance d from the DT fuel. The solid curves show E_{ig} versus T_p, for different values of d. The dashed curve is for monoenergetic protons. In all cases r_b = 15 m. (from Atzeni et al 2002).

Simulations of proton ignition of indirectly driven implosions of high gain fuel capsules (modeled in 1D) have been discussed by Temporal et al (2002)[12]. The proton beam is idealized as a cylindrical beam of radius 10 m. The target is imploded to a peak density

of 625 gcm^{-3} with a density minimum in the center. The proton beam has a temperature defined by an energy spectrum. The analysis shows that the ignition energy is not significantly increased when the 1D simulated density profile of the compressed fuel is used in the ignition calculation rather than a fuel mass of constant density.

A practically interesting geometry was also modeled in which it was assumed that a hemisphere implosion against a planar foil barrier could allow the source to hot spot distance for the proton beam from the other side of the planar foil to be as small as 500 m, bringing the ignition energy down to 10kJ. If the proton generating foil is also a hemisphere as has been used in the demonstrations of proton focusing discussed later, this configuration has obvious potential.

The laser energy required to produce the proton beam depends on the conversion efficiency and if that can exceed 10% as discussed later, the laser energy can be <100kJ and therefore competitive with the electron ignition option and in a feasible range of ignitor laser energy. The second critical requirement is that the focused beam delivers the energy into the required <50- m diameter ignition spot.

3. Proton beam generation

The first observation of a highly collimated very intense ionizing beam generated at the rear surface of thin foil targets irradiated with extreme laser intensity laser on the front surface, was reported by Key et al (1998)[13] based on images of the beam recorded on radio-chromic film in experiments using the first PW laser at the Lawrence Livermore National Laboratory. Initially the data were thought to indicate a collimated electron beam. Further study reported by Snavely et al., (2000)[14] and Hatchett et al (2000)[15]. Showed the previously observed beam to be protons with >10% of the laser energy converted to >10 MeV protons in a Boltzmann–like energy spectrum with a sharp cut off at about 58 MeV. Similar proton beams were observed in experiments with the 100TW Vulcan laser by Krushelnik et al., (1999)[16] and Clark et al., (2000)[17] and by Murakami et al., (2001)[18] using the 50 TW Gekko MII laser. Maksimchuk et al (2000)[19] observed proton beams of lower energy with a 10 TW laser. There was strong interest in the phenomenon and there followed many reports of proton beams observed at powerful short pulse laser facilities. Hatchett et al., (2000) and Wilks et al., (2000)[20] attributed the proton beam to hot electron pressure and a Debye sheath acceleration process creating a charge neutral free expansion of protons and electrons from the rear surface of the target in a fashion closely analogous to the well established study of fast protons generated from the front surface of targets irradiated at high laser intensities (Gitomer et al., (1986)[21], Sack and Schamell, 1982[22])

There was initially a vigorous debate about whether the proton beams originated predominantly from an alternative mechanism invoked originally by Krushelnik et al (1999) and Clark et al., (2000). This debate will not be reviewed in detail here as Borghesi et al discuss the general issues in proton beam generation in a companion paper in this special issue. There have been numerous publications giving evidence on the matter and it can now b e concluded that for laser intensities in the moderately relativistic

regime of interest for fast ignition ($3x10^{18} < I^2 < 3x10^{20} Wcm^{-2}$) the most energetic and collimated protons are generated in the sheath acceleration process at the rear surface of solid thin foil targets. A similar acceleration process also operates at the boundary of the laser-produced plasma on the irradiated front surface but the non-planar geometry of the plasma creates a wide angular pattern of acceleration with relatively poor collimation.

The rear surface sheath acceleration mechanism proposed by Hatchett et al (2000) is a particular case of the plasma free expansion mechanism accelerating protons from the front surface, which had already been extensively studied and analyzed particularly in connection with CO_2 laser experiments (see eg Mora 2003[23] for a recent improvement of the theory and referencing of the earlier work). The characteristic fast ion pulse seen in Faraday cup ion collectors was the experimental signature of that process (see for example collected fast proton data by Gitomer et al (1986)). The particular case considered here is different in one important detail, namely that that there is initially no plasma at the rear surface and a Debye sheath at the solid surface initiates the acceleration.

Efficient laser absorption mechanisms generate the electron source with typically >1MeV temperature similar to the ponderomotive potential $T_h \sim m_0 c^2 (\quad 1)$ where

$$= 1 + \frac{p_{os}^2}{2m_0^2 c^2}^{0.5} = 1 + \frac{I^2}{2.7x10^{18}}^{0.5}$$

See for example Wharton et al (1998) [24]. At relativistic energies the electron range greatly exceeds the thickness of target foils (typically $2 < t < 100$ m thick) and the electrons reflux between the front and rear surfaces as shown by Mackinnon et al (2002),[25] spreading laterally on each pass and establishing a radially spreading Debye sheath at the vacuum boundaries. The sheath potential set up by a small minority of the electrons traps the majority of the electrons in the target. The rear surface initially is not ionized .The sheath electric field at the surface which scales as the surface charge density , can be written as $2^{0.5} T/ _D$ and is proportional to $(N_e T_e)^{1/2}$ where $_D$ is the Debye length and N_e the hot electron density in the target. It sufficient to ionize the ubiquitous adsorbed water or hydro-carbon molecules attached as a mono-layer to the target foil.

Taking as an example PW laser experiments using a 300J, 0.5 ps laser pulse with about $3x\ 10^{20}$ Wcm^{-2} intensity in the laser focus, the average electron energy is roughly 3 MeV. Approximately 100J of hot electron energy is confined in the target. If we assume a typical volume of 100-mm-thickness x300 m diameter and neglect electron energy loss during the laser pulse, this gives an initial Debye sheath field of 1.7MeV/ m. The ionization creates a surface layer of extremely cold ions (H^+, C^{4+} etc). The lightest ions, the protons are accelerated most rapidly and the initial acceleration is perpendicular to the surface. If the surface is flat, the acceleration is highly collimated (Cowan et al 2004)[26]. There is an initial transient acceleration phase of duration equal to the inverse ion plasma frequency. This is followed by a self-similar expansion (velocity increasing approximately linearly with distance from the original surface) comprised of collisionless

charge neutral plasma of hot electrons and protons. Its scale length 1/n(dn/dx) increases at approximately the sound speed $(kT_h/2m_p)^{1/2}$ of cold protons and hot electrons. The Debye length increases as the electron density decreases. At some point towards the leading edge of the flow the local Debye length exceeds the density scale length. Charge neutrality breaks down at that point and the Debye sheath is located there with a lower charge density and electric field than that set up initially. The protons at the leading edge thus experience an E field, which diminishes in time, and there is a cut off in the maximum proton energy corresponding to the leading protons. The proton plasma following behind, in the self-similar expansion wave has a quasi-exponential density structure with lower velocity at higher density.

The second and quite different ion acceleration mechanism is light pressure at the reflection point (i.e. the critical density) which drives an electrostatic shock wave into the surface plasma formed by pre-pulse irradiation as discussed by Wilks et al., (1992)[27]. It acts on the electrons and causes them to drag the ions at the velocity of the light-pressure induced shock wave, of order $v=(P/\ )^{1/2}$, where P= I/c is the light pressure and the density . Wilks et al., considered the density to be the critical density, but more correctly it is the relativistically modified critical density N_{ec} . , See e.g. Pukhov et al (2001)[28]. The shock velocity is modest but as shown by Denavit (1992)[29] the highest proton energies are enhanced a factor of 4 by velocity doubling as protons bounce off the shock with energy $2 M_p v^2$ that is 8 MeV at 10^{20} Wcm^{-2}. The energy transfer efficiency is rather low at v/c (4.5% for this example). The directionality of this source is governed by the shape of the hole boring depression of the critical density which is typically strongly curved due to relativistic filamentation of the laser beam and related radial variations of the light pressure and relativistic changes to the critical density.

Evidence of this type of ion acceleration has been clearly seen in beam target fusion measurements where a laser drives deuterons into a cold CD target. Disdier et al (1999)[30] and Kodama et al (1999)[31] have reported experimental data and modeling analysis. A good discussion and modeling of the results of Disdier et al is presented by Toupin et al 2001[32] while Habara et al (2003)[33] report both experiments and modeling. At extreme intensities ($>>10^{21}$ Wcm^{-2}) the conversion efficiency to proton or other ion energy could be high (Esirkipov et al 2004 [34]). The mechanism is not however relevant for the proton fast ignition process considered here.

Helpful identification of the two mechanisms is provided by 2 and 3D PIC simulations such those of Murakami et al (2001) [18]and Pukhov et al (2001) [27] respectively. Both processes are illustrated by the particle in cell modeling by Murakami et al shown in figure (5) .The plot is from a 2D PIC simulation of a 5 micron thick DH target having a density 50x N_c, irradiated at $8x10^{18}Wcm^{-2}$ by a 400fs, 20J laser pulse. The proton momenta are plotted at the end of the pulse against their spatial position. The rear surface and front surface protons accelerated by the hot electrons are clearly seen as are the slower protons inside the target, accelerated by the light pressure driven shock. Plots of the plasma E fields and the electron momenta further confirm the physical picture as seen in figure 6 from Murakami et al.

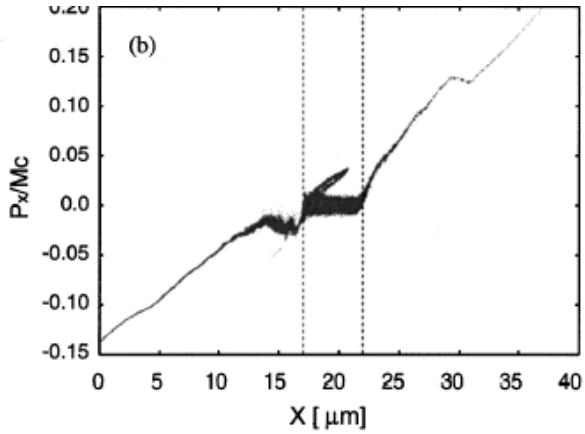

Figure (5) 2D PIC modeling of proton acceleration the plot shows the proton phase plot *X* vs. *P*+ at 452 fs. The dotted lines indicate the initial surfaces of the 5- m thick plasma at 40xcritical density. The irradiation was at $8x10^{18}Wcm^{-2}$ for 300 fs. (From Murakami et al (2001))

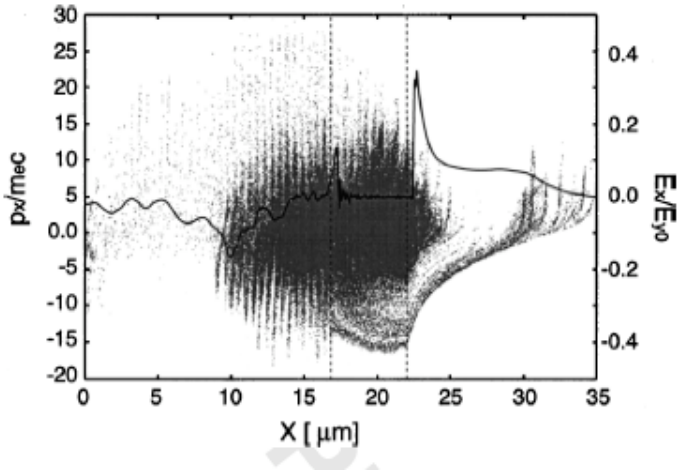

Figure 6 The electrons' phase plot *X* vs P_x at *t*= 132 fs for the simulation conditions of figure 5 The solid line is the time averaged longitudinal electrostatic field E_x in units of the transverse E field of the laser. (From Murakami et al 2001)

4. Energy spectrum of the proton beam

The ID theory with an infinite reservoir of hot electrons of fixed temperature such as in Mora's model [22] shows the E field at the Debye sheath diminishing with time due to falling density and the field scaling as $(NeTe)^{0.5}$. The maximum proton energy increases indefinitely but progressively more slowly (logarithmically) with time. In reality there is a finite source of hot electrons and they cool through collisions and adiabatic expansion, the latter becoming more rapid as the expansion changes from 1D to 3D. The acceleration is therefore truncated after some time, defining the cut off in the energy spectrum.

The energy spectrum below the cut off is associated with the near to exponential density structure of the self-similar free expansion into vacuum. The velocity increases with distance leading to an energy spectrum below the cut off energy, which Mora (2003) computes to have the form,

$$dN/d\mathcal{E} = (n_{i0}c_s t/\sqrt{2\mathcal{E}\mathcal{E}_0})\exp(-\sqrt{2\mathcal{E}/\mathcal{E}_0}),$$ Equation 2

Where E_o=kT, c_s is the sound velocity and n_{io} the initial density of protons (equal to the initial density of hot electrons and proportional to the laser energy for a given volume in the source foil).

The PIC modeling of Murakami et al. shows the slope temperature of the protons to be similar to the hot electron temperature and the cut off energy to be about 5x the electron temperature. There is some structure in the spectrum, including a slight peak near the energy cut off and another slight peak at intermediate energy arising from where the protons separate from the heavier ions. This structure in the energy spectrum has also been studied and modeled by Allen et al 2003[35]. The energy spectrum also varies with angle as discussed in the next section.

Experiments support the theoretical description with the cutoff energy and slope temperatures similar to the theoretical predictions, for example in the work of Snavely et al. (2000), MacKinnon et al (2001) and (2002). The highest cut off energy of 50 MeV and slope temperature of 4 MeV were observed with the most powerful laser in the 1PW experiments of Snavely et al (2000).

The LLNL Petawatt data are illustrated in figure 7. The bulk of the proton energy has a slope kT of approximately the 1~2 times the ponderomotive potential. The higher energy part of the proton distribution is almost flat on many shots with kT of 50-100 MeV and is always followed by a high-energy cutoff. Evident also is the softening of the proton spectrum with angle. Discussed in the next section.

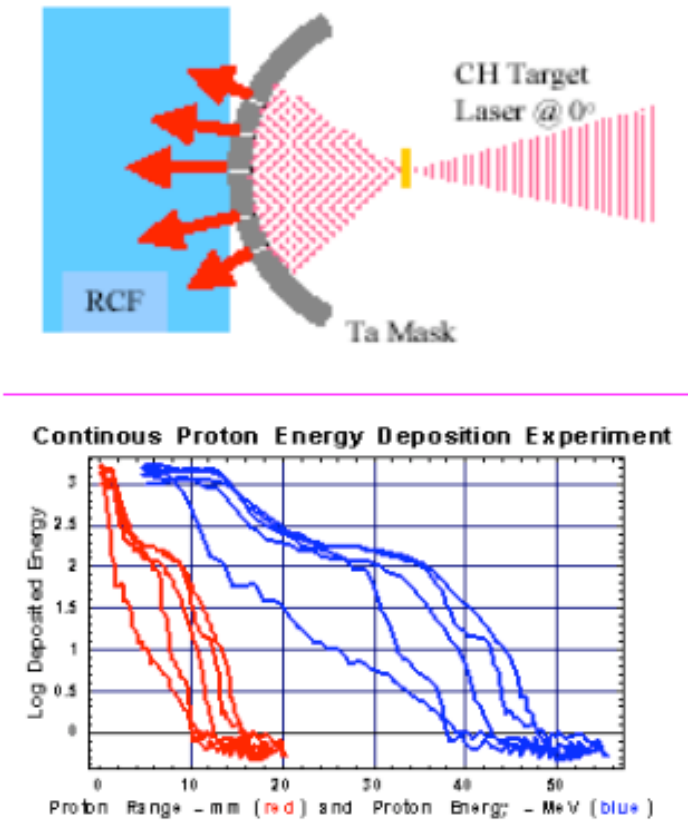

Figure 7 Proton spectrums of LLNL Petawatt shot 29042707. (Top) Schematic of the experiment (Below) Lineouts are taken along each of the beam paths in the radio-chromic film. Proton energies out to 48 MeV are evident, also diminishing range and energy with increasing angle. The RCF is saturated out to a depth of 14 MeV

5 Angular characteristics of the proton beam

The first radiochromic film pack images of the proton beam pattern, where higher proton energies are recorded in the deeper layers of the film pack, showed smaller circular beam patterns corresponding to lower beam divergence, at higher energies (Snavely et al 2000) illustrated in figure 8. Typical cone angles were 10^{o} at the highest energies increasing to $> 60^{0}$ at the lowest energies. The physics origin of this beam characteristic is simple in concept but complex in detail.

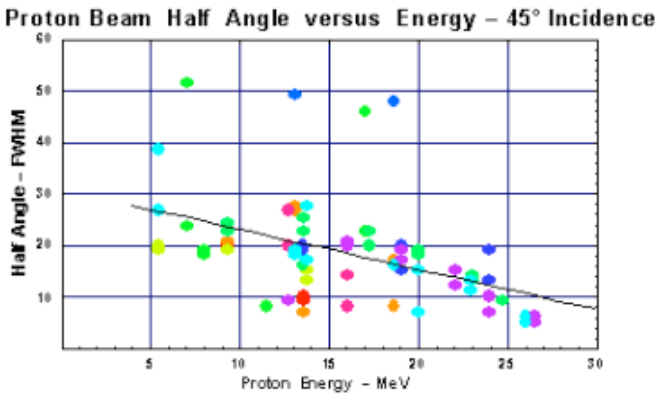

Figure 8 LLNL PW data (0 incidence) showing decreasing proton half angle with respect to proton energy. (Colors denote different shots) There is a consistent initial beam divergence of 25 for medium energy protons. On occasion, the beam divergence remains near constant until high energy. The difficult to measure (due to film saturation) low energy protons (E < 10 MeV) have very large initial beam angles.

An important factor is that the velocity of the expansion peaks at the center of the electron beam launched from the laser focal spot where the electron density and therefore the accelerating field are highest. The hot electron population also has an energy-angle relationship as discussed by Stephens et al.2003 [36], where lower energy electrons leave the laser focal region at greater angles than the higher energy part of the distribution. As the electrons spread radially their density is lower and they arrive later. The expanding Debye sheath therefore develops a bell shape with its peak at the center of irradiation. Since the acceleration is perpendicular to the sheath, the outer regions have a radial component of acceleration leading to a very characteristic feature of the proton beam in which the energy spectrum is a function of angle as seen in figure 7. The highest quasi - exponential slope temperatures and cut off energies occur on axis and at off axis angles these parameters decrease monotonically. The angles of the lower energy protons at the rear surface may also be further increased by the thermoelectric (fountain effect) magnetic field generated near to the rear surface. Murakami et al (2001) present both experimental data on the angle variation of the cut off energy and related PIC modeling which shows the influence of the rear surface fountain field on the angular pattern.

The divergence of the proton beam and its source size have been measured as a function of proton energy using a novel proton producing target incorporating diffraction grating-like grooves on its rear surface Cowan et al 2004[25]. The grooves imprint a pattern in the flow, which is seen in radio-chromic film– pack images of the proton beam. The source size of the proton beam is measured by counting the number of grooves across the RC picture and the angular divergence is given by the size of the image and the distance to the film.

The proton beam intensity patterns in the narrow energy bands defined by the Bragg peak stopping in stacks of radiochromic film, have been observed to range from uniform circles with a well defined edges to complex patterns with cusp like features. Uniform beams are seen with thick high Z foils and at lower intensities. The more complex patterns occur at higher intensities and in lower z and thinner foils. These characteristics can be attributed to variations in the density of electrons at the sheath due to resistive filamentation instability of the hot electron flux. The rear surface Debye sheath then has local variations in accelerating field and as the sheath expands at the leading edge of the plasma, complex topology develops rather than a simple bell shape. The topology induces local changes in the direction of acceleration of the protons, creating downstream flow intersections and characteristic cusp like- intensity patterns. These phenomena have recently been discussed by Fuchs et al. (2004)[37].

6. Conversion of laser power to proton beam power.

A crucial parameter for proton fast ignition is the efficiency of energy transfer from the laser to the proton beam. The primary transfer efficiency is that to the relativistic electrons, which can be as high as 50% (Yasuike et al 2001)[38]. A more complex process is the transfer from the electrons to the protons. In an ideal case where the only loss of electron energy is by adiabatic expansion, that transfer efficiency would be high. Collisional losses in the dense foil target provide an additional loss channel, as does Bremsstrahlung radiation. The ratio of energy transfer to protons from the front surface relative to that at the back is another factor.

High efficiencies of energy transfer to protons (>60% of the absorbed laser energy) from a spherical glass microballoon target have been observed using multi-kJ, nanosecond pulses at 10.6 micron wavelength. (Hauer et al. 1984[39]). This is however a very different regime than we are concerned with here.

PIC modeling does not give a very good basis for determining the absolute efficiency because it does not treat collisional and radiation losses in the high-density foil.

Experimental data on the conversion efficiency into rear surface proton beams is rather sparse but intriguing because it shows conversion efficiency increasing with laser energy and reaching levels close to 30%. Data from Snavely et al 2000, MacKinnon et al 2001 and Mackinnon et al 2002 obtained with 400 J, 50 J and 10 J laser pulses respectively are plotted in figure 7. In order to make this comparison the published data of Snavely et al on conversion to protons of >10 MeV energy have been scaled to compare with the other two publications using the cut-off energy and slope temperature to infer the total energy in a Maxwellian spectrum.

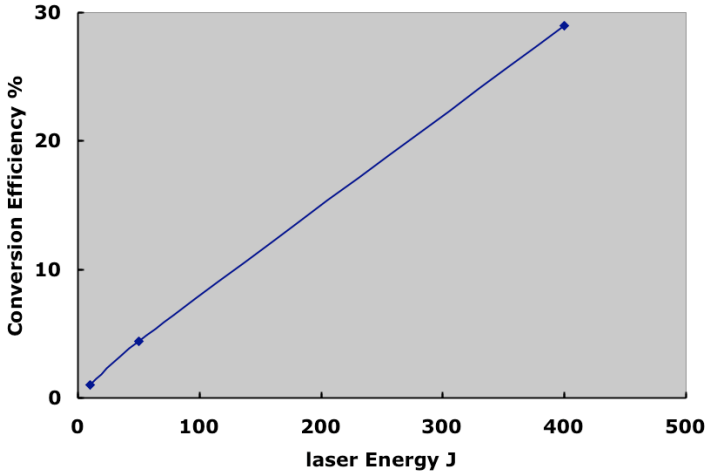

Figure 7 Conversion efficiency into a Maxwellian energy spectrum inferred from the absolute number of protons per energy interval at energies >10 MeV and the slope temperature (data from 3 experiments discussed in the text).

The efficiency of rear surface proton production has not previously been analyzed but it is of crucial importance for fast ignition where very high laser energy must be used and efficiencies >10 % are needed. The high efficiency obtained in the PW experimental data in figure 7 meets the requirement. From physics perspective the efficiency is determined by competition between electron energy dissipated adiabatically in proton acceleration at the rear surface and that dissipated in acceleration at the front surface and collisionally in the proton source foil.

The rate of transfer of energy to the protons initially increases from zero in a transient acceleration phase of duration equal to the inverse ion plasma frequency. It peaks at the level associated with the self-similar expansion computed for example by Mora (2000). His solution for the power scales linearly with electron density in his expression for the proton energy spectrum given previously as equation 2. The time scale for energy transfer to the proton plasma is therefore independent of the laser energy. The time scale for an electron to lose energy by collisions in the solid density foil is also independent of the total number of electrons and is therefore independent of the laser energy. Thus the ratio of the two time scales is constant implying no energy dependence of the conversion efficiency in contradiction to the data in figure 7.

The explanation of the reduced efficiency at low energy may be found in the transient phase of the expansion. At low energies the electron density is low and the corresponding proton ion plasma frequency is also low scaling as $(\text{density})^{0.5}$
The transient phase during which the power into the proton beam increases from zero to the steady state level, is therefore of longer duration and can exceed the collision damping time of the electron energy causing a reduction in conversion efficiency.
Regarding the power flow from the front relative to the back surface it appears that the ubiquitous preformed plasma on the front surface will have a scale length much greater

than the Debye length corresponding to the hot electron density, thereby significantly reducing the accelerating field and power flow from the front relative to the back. Deliberate creation of preformed plasma on the back has been shown to drastically reduce the proton beam power by MacKinnon et al (2001)[40]

More carefully controlled experiments are needed togther with more detailed analysis to fully understand this important efficiency issue. The discussion here suggests that efficiency may be optimized by maximizing the hot electron density and minimizing the collisional loss by using thin low z foils of limited area and high laser energy.

7. Focusing of the proton beam and isochoric heating

The exceptionally low transverse temperature of the proton source (see the recent discussion by Cowan et al (2004) [25]) and its well-defined flow pattern lead to the possibility of using a concave surface to focus the flow. This was recognized soon after the discovery of the proton beams and motivated the first PIC modeling which demonstrated the focusing effect by Wilks et al (2001)[20], and the proposal of proton fast ignition by Roth et al[10]. Ideally a homogeneous hot electron density causes the protons from a hemisphere surface to focus at its centre as seen in the PIC modeling by Wilks et al. Early attempts to observe focusing with rather weakly curved surfaces were not successful. Consideration of the typical angular divergence of the proton beam associated with the bell shaped Debye sheath discussed previously, suggested that for effective focusing, the concave surface curvature must be much stronger than the observed divergence of the proton flow from a planar target. This led to the successful use of a very strongly concave hemispherical shell to focus the protons by Patel et al (2003)[41]

The experiment illustrated in figure (8) used an Al hemisphere fabricated with a very smooth inside surface, a diameter of 320 μm and a thickness of 10 μm. The hemisphere was irradiated on its pole with a 100 TW 100 fs laser focused to a 50- m diameter. A 15-μm thick planar Al foil was located at the equatorial plane. Heating by a proton beam is strongly dominated by those protons at the end of their range because of the strong Bragg peak in proton energy deposition. Protons of 0.9 MeV have 10- m ranges in Al and dominated the heating of the Al foil. Streak camera time resolved imaging of the Planckian thermal emission from the foil showed from the absolute intensity, that a 50- m region was heated to 20 eV temperatures. Substituting two planar foils showed a 5x-reduced temperature and heating over a larger 200- m region. When a single foil was irradiated the rear surface heating due to electrons was almost an order of magnitude less than was produced by the same laser pulse generating focused protons.

Extension of the technique to heating by protons of higher energy up to 3 MeV and closer to the requirement in fast ignition, was accomplished in an experiment with a much higher energy 200J, 1ps laser (the Gekko PW laser in Japan) and similar hemisphere shells projecting a proton beam onto Al foils up to 100 m thick. In this work XUV imaging of the rear surface Planckian emission was used to show the spatial pattern of heating and the temperature was deduced from the time integrated absolute intensity in

conjunction with radiation/hydrodynamic modeling of the explosive expansion of the heated region. Time resolved UV images provided a second measure of the Planckian emission and the temperature. The rear surface temperature was highest for the thinnest targets, reflecting the quasi–exponential proton energy spectrum and target variation with target thickness of the Bragg peak proton energy. Temperatures ranged from 25 eV at 100-mm thicknesses to 90 eV at 10 m. The heated region was once again of about 50-micron diameter. An interesting additional observation was intense x-ray emission in a pinhole camera image of the front surface of the proton target foil-indicating proton heating to a few hundred eV. The variation of temperature with axial location of the rear surface of the foil showed optimum heating at about 1.7R rather than at 1R illustrating that the intrinsic divergence of the protons displaces the plane of optimum focusing. (Snavely et al (2004)[42]. We have recently extended the data of Snavely et al in experiments with 400 J, 1 ps pulse at the Vulcan PW laser in the UK.

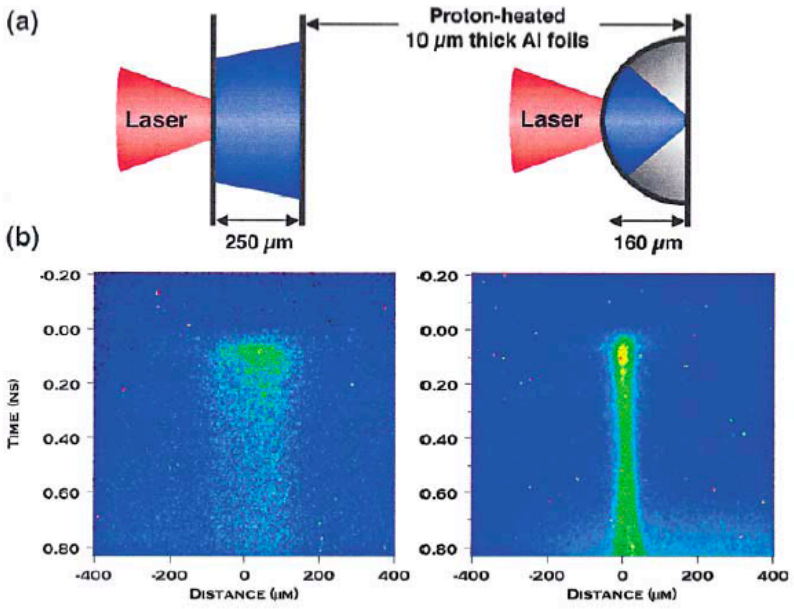

Figure 8. Proton focusing demonstrated by Patel et al (2003). Images in (b) show the spatially and temporally resolved thermal radiation emitted from the rear surface of a proton-heated 10 μm thick Al foil.

The focusing can be understood from the source size and cone angle relationship in proton beam generation from a planar foil, which indicates a quasi-spherical flow with an almost linear proportionality of source size and cone angle equivalent to the effect of a diverging lens. . There is also an inverse proportionality of cone angle and energy. The flow from a concave surface can be estimated by re-computing the flow angles, adding the measured divergence as a function of radius to the normal to the surface. Such an analysis[43] predicts the axial position of best proton focusing in agreement with experiment of Patel et al and the more recent data of Snavely et al.

This geometrical approach is however rather simplistic and it neglects another feature of the proton flow revealed in the grooved target data. As discussed earlier the groove patterns at lower energies are seen to fade rapidly in visibility in the direction perpendicular to the grooves. This indicates shear in the flow associated with a bell shaped accelerating sheath with wide flat wings. Acceleration of low energy protons in the wings is consequently near to normal to the surface and the flow lines from larger radii cross with the those from smaller radii where the bell shape has maximum slope. The shear washes out the groove pattern for directions perpendicular to the grooves but not parallel to them. On this basis it is seen that the proton focusing has 'aberrations'. A corollary of the aberrated focusing from a sphere is that it may be possible to shape the surface to compensate for some of the aberrations. Another factor not understood at present is the possible modification of the focusing by the internal pressure of the high density of protons in the focus.

More sophisticated modeling is necessary to describe the focusing with good accuracy. Both 3D explicit PIC modeling and 3D implicit hybrid PIC modeling are being developed to provide this better description which will be important for the future exploration of proton fast ignition. The most developed at present is explicit 3D PIC modeling by Ruhl et al (2001)[44] using the PSC code as illustrated in figure 9

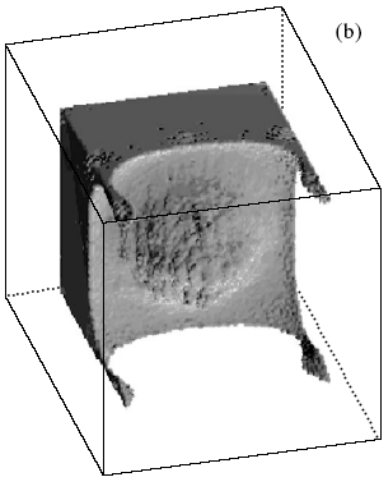

Figure 9 3D PIC model of proton focusing in a 30x30x40 μm simulation box with a hemisphere shell of radius 22 μm, thickness 5 μm and density 1.6×10^{21} cm^{-3} irradiated at 10^{21} Wcm^{-2} with a 70 fs pulse. The plot shows the formation of the bell shaped proton flow after 200 fs.(from Ruhl et al. 2001)

The limitations of 3D explicit PIC modeling are the low density, short time and small volume of the calculation. Larger scale calculations are possible in 2D as illustrated by further work with the PSC code reported by Patel et al (2003). Figure 10 shows an electric field density map from a calculation of a 5×10^{18} Wcm^{-2} laser pulse incident on a 250 μm diameter, 10 μm thick Al shell. A 0.1 μm H layer is added to the inner surface to

simulate the hydrocarbon layer generating the protons. A bell shaped ion front is observed approaching a second 10 μm thick planar foil located at the center of the hemisphere.

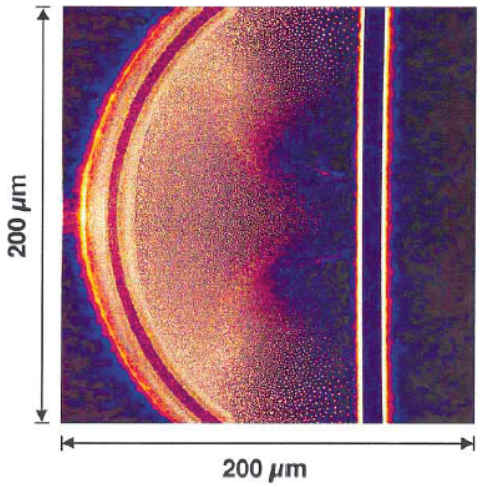

Figure 10 Proton focusing modeled by 2D explicit PIC on the spatial scale of experiments. Particle-in-cell calculation of the electric field density at 3.4 ps for a $5x10^{18}$ Wcm^{-2} intensity laser pulse incident on a 250 m diameter, 10 m thick hemispherical Al shell. (from Patel et al.(2000)).

8. Physics of isochoric heating by protons

The previously described experiments on proton focusing have demonstrated isochoric heating of solid density matter to temperatures>100eV. The physics of the heating process itself is at an early stage of investigation.

The stopping of protons is well documented and a good discussion is given by Melhorn (1981)[45]. In cold matter the energy loss is to ionization of bound electrons. There is a pronounced peak in energy loss at the end of the range and this Bragg peak results in heating at any depth in a target being predominantly by a narrow energy band of protons near to the end of their range (see e.g. Hatchett et al (2000) [15]). It follows that in a quasi-exponential spectrum; heating will diminish rapidly over depth ranges such that the change in proton energy at the Bragg peak is large compared to the axial temperature of the beam. In general the proton energy loss rate is also a function of the temperature of the heated material. The loss rate decreases with temperature as discussed previously, for protons in DT where the loss is to free electrons. Energy loss rates in other materials vary differently because they are the combined with the effect of loss to both free and bound electrons. For example in the experiments on proton heating of Al discussed previously the energy loss rate increases by about factor of two to a maximum at a temperature of about 100 eV, then decreases at higher temperatures, equaling the cold Al loss rate at a temperature of about 500eV. Rutherford scattering from nuclei adds some divergence to

the proton beam but this is generally insignificant relative to the dynamics of the focusing in determining the dimensions of the heated region.

Due to the presence of the neutralizing, co-moving population of electrons, the proton beam is more correctly described as a plasmoid. When the beam reaches the dense target to be heated it consists of ballistically focused protons accompanied by the neutralizing electrons. The electrons have a high temperature initially but this diminishes as the plasmoid expands. The electrons reflux within the proton generating foil and the expanding proton plasmoid they lose energy collisionally in the dense foil and by adiabatic cooling as they do work to drive the expansion of the plasmoid and most of the energy of the plasmoid resides with the protons when the beam reaches the target. When contact is made with a target the protons entering the target must still be accompanied by neutralizing electrons. The electrons may penetrate the target more rapidly than the protons as in the previously discussed electron isochoric heating. The relative effects of electrons and protons depend on the electron temperature. For situations of interest the electron temperature will generally be low enough that the energy transport is by protons. A test of this was carried out in the work of Snavely et al 2003 and it was observed that there was no detectable electron excited K fluorescence from a Cu layer in the Al target heated by proton focusing.

The possibly non-linear behavior of the protons in the target is at an early stage of study. Ruhl et al. (2004)[46] have used PIC modeling of an intense proton beam (10 m diameter, 15MeV, 10^{21} /cc, with accompanying 100keV electrons) entering a low-density cool proton plasma (10^{21}/cc, 1keV). Their results show a non-linear interaction triggered where the beam density exceeds the background density, with pinching and subsequent divergence of the beam due to a break down of current neutralization through a two-stream instability of the electrons. More work is needed to understand how non-linear effects may influence a full-scale proton fast ignition.

9. Practical constraints on proton fast ignition and a conceptual design.

A number of practical considerations are important when considering the feasibility of proton fast ignition.

The proton producing foil target must be irradiated at an appropriate intensity to create a proton beam in the optimum temperature range of 2-5 MeV. Experiments and theory suggest an intensity of about 10^{20}Wcm^{-2}. The radius of the focusing foil should be as small as possible to minimize the transit time spread and therefore the ignition energy. The laser must deliver the required energy in a pulse shorter than the inertial confinement time of about 20 ps. Pulses of shorter duration for a given energy require larger final optical aperture in the laser so the pulse should be as long as possible. The need to complete the proton acceleration before the closure of the accelerating vacuum gap constrains the minimum radius and maximum pulse length.

A scenario, which might be feasible, would use 1 mm radius consistent with the previously discussed 16kJ ignition energy. With a laser pulse of 100kJ in 3ps, 200 m diameter focal spot gives the required 10^{20}Wcm^{-2} intensity. If the accelerating hemisphere is 10 m thick Cu and the hot electrons reflux in the shell they have an average density of 4.5×10^{20} cm^{-3}. 30 % absorption and a 50:50 partition of energy between heating the shell and proton acceleration raises the shell temperature to about 200eV and delivers the required 17kJ of protons. The 1mm gap closure time following the model of Mora (2002) is 8 ps and thus a sufficiently longer time than the duration of the laser pulse.

A crucial factor is the spot size of the proton beam. The experiments discussed in section 8 showed heated regions down to 50- m diameters with 190- m radius hemispheres. If the focusing were self-similar there would be a 300 m focal spot with a 1 mm radius. Ignition requires a 40- m spot and so this scenario would not ignite. It may be possible to shape the surface of the shell to correct for the non-sphericity of the ballistic focusing as discussed previously but this has not yet been shown to be possible. It is clear that this is one area where much more work is required.

The 200- m laser focal spot is a major potential advantage for proton fast ignition relative to electron ignition because it is consistent with an extremely long focal length of the final focusing optic. For example using beams similar to the NIF laser at 40 cm diameter and equating 200 m to be 3 times the 1st minimum of a diffraction limited spot gives an f/38 optic with a focal length of 15m. Such a large stand off distance and weak convergence angle would be of great practical value in a fusion power plant delivering the ignition energy via a cluster of say 30 beams of 40 cm diameter. A further advantage of this scenario is that it bypasses the limit in electron fast ignition where the intensity required in the electron beam implies a laser intensity so high that the generated electron energies would be too penetrating for efficient coupling of energy to the hot spot by electrons.

The fraction of a hemisphere used must also be optimized. The configuration could be a hemispherical compression onto a planar barrier with a hemisphere proton-focusing target on the opposite side. Alternatively the proton beam could be generated in a sub –hemisphere cone as in figure 2, with an implosion around the cone as used in the first demonstrations of integrated fast ignition. To date it has not been verified that the proton generation mechanism is effective in such restricted cone geometry.

It has been shown that a pre -formed plasma of significant scale length on the rear surface of the target quenches proton beam generation (MacKinnon et al (2001)). The proton source foil must therefore be protected from pre- plasma formation due to particle or photon fluxes from the compression event. This requires either sufficient barrier thickness or mass that no significant radiation penetrates or shock break through occurs before the protons are generated. An interposed protection foil between the compression event and the proton generating foil may be required in addition to the protection afforded by the walls of the cone. The protons must then traverse these barriers before they reach the ignition hot spot. The effect of a vacuum gap has not yet been studied.

10. Conclusions

In summary proton fast ignition is an interesting and newer approach to fast ignition which could avoid problems in electron fast ignition arising from the strong self generated E and B fields on particle energy transport process and the lack of self consistency in the laser intensity requirements for optimum electron energy and for ignitor electron beam intensity. The early stage of the research on many aspects of proton fast ignition makes its prospects intriguing but uncertain until more work is undertaken. In particular achieving the required conversion efficiency at the full FI energy and the small diameter of the focused beam appear to be the major challenges.

Acknowledgements

We are grateful to our collaborators in the early stages of this research, particularly M Roth and S C Wilks and TC Cowan also to R Kodama and K A Tanaka for their collaboration in proton heating studies at the Gekko PW laser facility, to our many collaborators in large scale multi- purpose experiments at the Rutherford Laboratory Vulcan PW laser which included studies of proton heating and to H Ruhl for his collaboration and insightful modeling of proton focusing and heating .

11. References

[1] J D Lindl Phys Plasmas 2 3933 (1995) and Phys Plasmas 11 339 (2004)
[2] S E Bodner et al. Phys Plasmas 5, 1901 (1998)
[3] N.G. Basov, S.Y. Guskov and L.P. Feokistov, *J. Sov. Laser Res.* **13**, 396 (1992).
[4] M Tabak et al Phys Plasmas 1 1626 (1994)
[5] S Hatchet et al presentation given at Anomalous Absorption meeting, Ocean City, MD USA (April 2000).
[6] R Kodama et al Nature 412,798 (2001) and R K Kodama et al. Nature 418, 933 (2002)
[7] M H Key Nature 412, 775 (2001)
[8] S Atzeni Phys Plasmas 6 3317 (1999)
[9] M H Key et al J Fusion Energy 17, 231 (1998)
[10] Roth *et al.*, Phys. Rev. Lett. **86**, 436 (2001)
[11] S Atzeni M Temporal and JJ Honrubia Nucl Fusion 42 L1 to L4 (2002)
[12] M Temporal, J J Honrubia, S Atzeni, Phys Plasmas 9, 3098, (2002)
[13] M H Key et al J Fusion Energy 17, 231 (1998)
[14] R A Snavely et al. Phys Rev Letts 85, 2945 (2000)
[15] S J Hatchett et al. Phys Plasmas 7, 2076, (2000)
[16] K Krushelnik et al Phys Plasmas, 7,2055, (1999)
[17] E. L. Clark *et al.*, Phys. Rev. Lett. **84**, 670 (2000).
[18] Y. Murakami *et al.*, Phys. Plasmas **8**, 4138 (2001).
[19] A Maksimchuk et al Phys Rev Lett. 84, 4108 (2000)
[20] S C Wilks et al Phys Plasmas 8, 542 (2001)
[21] S. J. Gitomer et al. Phys. Fluids **29**, 2679 (1986)
[22] Sack and Schamell Physics reports **156**,6, 311-395 (1987)
[23] P Mora Phys. Rev. Lett, 90, 185002, (2003)
[24] K Wharton et al. Phys Rev Lett.81, 822, (1998)
[25] A J. MacKinnon *et al.*, Phys. Rev. Lett. **88**, 215006 (2002).
[26] T E Cowan et al . Phys Rev Lett. 92, 204801 (2004)
[27] S C Wilks et al, Phys Rev. Lett. 69, 1383(1992)
[28] A Pukhov, Phys Rev Lett. 86,3562,(2001)
[29] J. Denavit, Phys. Rev. Lett. **69**, 3052 (1992).
[30] L. Disdier, J. -P. Garc¸onnet, G. Malka, and J. -L. Miquel, Phys. Rev. Lett. **82**, 1454 (1999)

[31] Kodama, K. A. Tanaka, T. Yamanaka *et al.*, Plasma Phys. Controlled Fusion **41**, A419 (1999).
[32] C Toupin E Lefebvre and G Bonnaud. Phys Plasmas. 8,1011. (2001
[33] H Habara et al. Phys Plasmas 10 3712, (2003)_
[34] T Esirkipov et al. Phys Rev Lett. 92, 175003 (2004)
[35] M Allen et al Physics of Plasmas, 103283, (2003)
[36] R.B. Stephens et al. Phys. Rev E. 69, (2004)
[37] J Fuchs et al. Phys Rev Lett. 91,255002, (2004)
[38] K Yasuike et al. Rev. Sci. Instr. 72,1236, (2001)
[39] A Hauer et al. in Laser Interaction and related Plasma Phenomena Eds H Hora and G Miley. Publ. Plenum Press, New York p. 479 (1984)
[40] A. J. MacKinnon et al. Phys Rev Lett. 86, 1769, (2001)
[41] P K Patel et al Phys Rev Lett., 91, 125004 (2003)
[42] R.A. Snavely et al., in Inertial Fusion Science and Applications 2003 Proceedings (Pub. American Nuclear Society Inc, p. 349. (2004)
[43] M H Key. A model of the focusing of laser generated proton beams. NIF Report Dec 2002
[44] H Ruhl et al. Plasma Phys Rep. 27, 363, (2001)
[45] T Mehlhorn, J Appl. Phys. 52,8522, (1981)
[46] H Ruhl et al. Nucl Fus. 44, 438, (2004)
A. J. MacKinnon *et al.*, Phys. Rev. Lett. **86**, 1769 (2001).
Sack an Schamell Phys. Reports, **156**, 313 (1987).